Conformational Analysis of 4,1′,6′-Trichloro-4,1′,6′-trideoxy-*galacto*-sucrose (Sucralose) by a Combined Molecular-Modeling and NMR Spectroscopy Approach

Christophe Meyer,† Serge Pérez,*,† Catherine Hervé du Penhoat,‡ and Véronique Michon‡

Contribution from Ingénierie Moléculaire, Institut National de la Recherche Agronomique, BP527, 44026 Nantes, France, and Laboratoire de Chimie de l'Ecole Normale Supérieure, 24 rue Lhomond, 75230 Paris, France

Received November 23, 1992®

Abstract: Sucralose, a trichlorinated derivative of sucrose (4,1′,6′-trichloro-4,1′,6′-trideoxy-*galacto*-sucrose), is approximately 650 times sweeter than sugar on a mass basis. It has a sucrose-like taste profile, with no unpleasant aftertaste, while being noncaloric and noncariogenic. This sweetener is emerging as the most commercially useful compound in the field of sucrochemistry. The conformational behavior of aqueous sucralose was studied by NMR and computerized molecular modeling. Steady-state NOEs at 400.13 MHz and transient NOEs at both 250.13 and 400.13 MHz have been measured. Long-range $^{13}C-^{1}H$ coupling constants are also reported. In parallel, the complete conformational analysis of the disaccharide has been achieved with two different molecular mechanics methods. The conformation of the pyranose ring is confirmed by the excellent agreement between the experimental and theoretical intracyclic scalar coupling constants. The furanoid ring is shown to exhibit some flexibility, covering the four adjacent ${}_3E$, ${}^4T_3$, ${}^4E$, and ${}^4T_5$ shapes. Within the potential energy surfaces calculated for the disaccharide, four families of stable conformers can be identified. One of these corresponds closely to the crystalline conformation of sucralose not only in terms of conformation about the glycosidic linkage but also in terms of orientation of the chloromethyl groups and occurrence of the interresidue hydrogen bond. The $^3J_{C-H}$ coupling constant about the glycosidic linkage was calculated using an equation suitable for COCH segments. The data do not support a single conformational model, and only conformational averaging can provide agreement between theoretical and experimental parameters. The theoretical NMR relaxation data were calculated taking into account all the accessible conformations and using the averaging methods appropriate for both slow and fast internal motions. In agreement with a recent solution dynamics simulation of β-maltose, the relaxation data suggest that the large-amplitude interglycosidic torsional motions of sucralose are occurring on a time scale similar to that of molecular reorientation. This extensive molecular-modeling investigation provides a good description of the conformational behavior of both aqueous and crystalline sucralose.

Introduction

The quest for the hedonic delight of sweet taste sensation without caloric intake has stimulated research on finding an alternative to sucrose with no side or aftertaste effects. Since sweet taste is exhibited by a large number of compounds from diverse structural classes, target molecules have included modified sucroses and various glycosides, peptides and proteins, flavonoids, saccharin, acesulfam, etc.

In the field of sucrochemistry, the discovery of an intensely sweet chloro sugar[1] has initiated studies on chemical modification of sucrose by halogenation. Several mono-, di-, tri-, and tetradeoxy halogeno derivatives have been shown to enhance sweetness by up to several thousand times.[2] Of these molecules, 4,1′,6′-trichloro-4,1′,6′-trideoxy-*galacto*-sucrose (sucralose) has emerged because of both its sweetness quality and its stability to the processing and storage conditions required by the food industry. It is not metabolized in the body and is noncariogenic. The molecular conformation in crystalline anhydrous sucralose is known from X-ray[3] diffraction studies; the description of its conformational behavior has been probed by ^1H SIMPLE NMR studies,[4] infrared[5] and Raman[6] investigations, and molecular-modeling calculations.[7] However, a unified interpretation of the conformational features of sucralose is still lacking. This is of particular interest for further investigation of structure–activity relationships of sweet molecules.

The present study describes the conformational behavior of sucralose as assessed through high-resolution NMR spectroscopy and extensive computerized modeling using molecular mechanics calculations. Inevitably, this study is implicated in the controversy about the solution conformation of sucrose.[8-13] In particular, attention has been drawn to the difficulties inherent in the interpretation of results from NMR relaxation studies in the presence of internal motion and strong coupling.

* Author for correspondence.
† Ingénierie Moléculaire, Institut National de la Recherche Agronomique.
‡ Laboratoire de Chimie de l'Ecole Normale Supérieure.
® Abstract published in *Advance ACS Abstracts*, October 1, 1993.

(1) Hough, L.; Phadnis, S. P. *Nature* **1976**, *263*, 800.
(2) Hough, L.; Phadnis, S. P.; Khan, R.; Jenner, M. R. UK Patents 1 543 167 and 1 543 168, 1979.
(3) Kanters, J. A.; Scherrenberg, R. L.; Leeflang, B. R.; Kroon, J.; Mathlouthi, M. *Carbohydr. Res.* **1988**, *180*, 175–182.
(4) Christofides, J. C.; Davies, D. B.; Martin, J. A.; Rathbone, E. B. *J. Am. Chem. Soc.* **1986**, *108*, 5738–5743.
(5) Mathlouthi, M.; Seuvre, A-M.; Birch, G. G. *Carbohydr. Res.* **1986**, *152*, 47–61.
(6) Mathlouthi, M.; Portmann, O. *J. Mol. Struct.* **1990**, *237*, 327–338.
(7) Hooft, R. W. W.; Kanters, J. A.; Kroon, J. *J. Comput. Chem.* **1991**, *12*, 943–947.
(8) Bock, K.; Lemieux, R. U. *Carbohydr. Res.* **1982**, *100*, 63–74.
(9) McCain, D. C.; Markley, J. L. *J. Am. Chem. Soc.* **1986**, *108*, 4259–4264.
(10) McCain, D. C.; Markley, J. L. *J. Magn. Reson.* **1987**, *73*, 244–251.
(11) Kovacs, H.; Bagley, S.; Kowalewski, J. *J. Magn. Reson.* **1989**, *85*, 530–541.
(12) Hervé du Penhoat, C.; Imberty, A.; Roques, N.; Michon, V.; Mentech, J.; Descotes, G.; Pérez, S. *J. Am. Chem. Soc.* **1991**, *113*, 3720–3727.
(13) Poppe, L.; van Halbeek, H. *J. Am. Chem. Soc.* **1992**, *114*, 1092–1094.

0002-7863/93/1515-10300$04.00/0

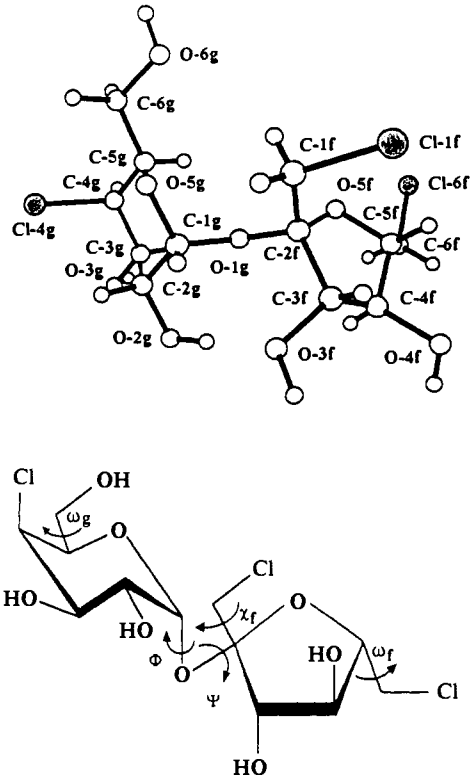

Figure 1. (a, top) Perspective view of sucralose along with the atom labeling; the chlorine atoms are shaded. (b, bottom) Sucralose with the torsion angles of interest.

Materials and Methods

Materials. Sucralose was obtained according to a literature procedure.[14] Solutions of this compound were prepared in D_2O (99.96%, SST).

Nomenclature. The labeling of the atoms and the torsional angles of interest are represented in Figure 1. Flexibility around the glycosidic linkage bonds is described by the following two torsion angles:

$$\Phi = (\text{O-5g–C-1g–O-1g–C-2f})$$

$$\Psi = (\text{C-1g–O-1g–C-2f–O-5f})$$

Another angle of interest is the glycosidic valence angle C-1g–O-1g–C-2f.

Conformational variations of the hydroxymethyl and the two chloromethyl groups are described by the torsion angles ωg, ωf, and χf:

$$\omega_g = (\text{O-5g–C-5g–C-6g–O-6g})$$

$$\omega f = (\text{O-5f–C-5f–C-6f–Cl-6f})$$

$$\chi f = (\text{O-5f–C-2f–C-1f–Cl-1f})$$

The three staggered orientations of the galactopyranosyl primary hydroxyl group are referred to as either *gauche–gauche* (GG), *gauche–trans* (GT), or *trans–gauche* (TG) with respective values of –60°, 60°, and 180°. In this terminology the torsion angle (O-5–C-5–C-6–O-6) is stated first and (C-4–C-5–C-6–O-6) second. The same convention was adopted for the Cl-6f fructofuranosyl chloromethyl group, whereas (O-5f–C-2f–C-1f–Cl-1f) and (C-3f–C-2f–C-1f–Cl-1f) were used for the remaining chloromethyl group. The sign of the torsion angles is defined in agreement with the recommendations of the IUPAC–IUB Commission of Biochemical Nomenclature.[15]

The nonplanar character of the galactopyranosyl residue can be described quantitatively by the Cremer and Pople ring-puckering parameters[16] Q, θ, and ϕ. In this terminology, Q is the total puckering amplitude, θ an angle expressing the deviation from an ideal $^4C_1$ chair, and ϕ the phase of pseudorotation. For the fructofuranosyl residue the position and extent of puckering (ϕ, Q) are sufficient to describe the distortion of the five-membered ring.

NMR Spectroscopy. ^1H (250.13 and 400.13 MHz) and ^{13}C NMR (100.6 MHz) spectra were recorded with Bruker instruments operating in the Fourier-transform mode at 296 K unless stated otherwise. The vicinal coupling constants, $^3J_{H,H}$, were extracted from a spectrum with a digital resolution of 0.12 Hz/point. The proton spectra of the galactosyl and fructofuranosyl residues of sucralose were simulated individually with the Bruker software package PANIC and then summed. The strong coupling parameters of the methylene protons were calculated with the following equation:

$$S = \sin 2\theta = [1 + (\Delta\delta/J)^2]^{-1/2}$$

where $\Delta\delta$ is the frequency difference ($\omega_A - \omega_B$) and J is the scalar coupling constant of the strongly-coupled spins.

Both ^{13}C and ^1H T_1 measurements were acquired with the inversion–recovery sequence (180–τ–90–FID), and relaxation times were calculated with the Bruker T_1 routine. The determination of selective ^1H relaxation times required soft 180° pulses (20 ms), which were performed with the DANTE[17] sequence. In the case of the rigid-molecule calculations, the overall tumbling was calculated from the average value of the methine carbon T_1s as follows:

$$\frac{1}{T_1} = \frac{\hbar^2\gamma_C^2\gamma_H^2}{10r^6}\left(\frac{\tau_c}{1+(\omega_H-\omega_C)^2\tau_c^2} + \frac{3\tau_c}{1+\omega_C^2\tau_c^2} + \frac{6\tau_c}{1+(\omega_C+\omega_H)^2\tau_c^2}\right)$$

where $\hbar$ is Planck's constant divided by 2π, r is the carbon proton internuclear distance (1.12 Å),[9,18] and γ_C and γ_H are the carbon and proton magnetogyric ratios. For the flexible-residue calculations the overall tumbling was evaluated from the average value of the methine carbon T_1 values as follows:[19]

$$\frac{1}{T_1} = K\left(\frac{\bar{S}_2\tau_c}{1+a\tau_c^2} + \frac{(1-\bar{S}^2)\tau}{1+a\tau^2} + \frac{3\bar{S}^2\tau_c}{1+b\tau_c^2} + \frac{3(1-\bar{S}^2)\tau}{1+b\tau^2} + \frac{6\bar{S}^2\tau_c}{1+c\tau_c^2} + \frac{6(1-\bar{S}^2)\tau}{1+c\tau^2}\right)$$

where $K = \hbar^2\gamma_C^2\gamma_H^2/10r^6$, a–c are the transition frequencies ($\omega_H - \omega_C$, ω_C, and $\omega_H + \omega_C$), and τ_e ($\tau^{-1} = \tau_c^{-1} + \tau_e^{-1}$) is the correlation time of the internal motion.

The correlation times of individual protons were evaluated from the ratio of nonselective to selective relaxation times according to Mirau et Bovey:[20]

$$\frac{T_1^S}{T_1^{NS}} = \frac{24\omega^2\tau_H^3 + 15\tau_H}{10\tau_H + 23\omega^2\tau_H^3 + 4\omega^4\tau_H^5}$$

Three-bond heteronuclear coupling constants were determined with a modified version[21a] of the semiselective two-dimensional INEPT sequence.[21b,c] The selective 180° ^1H pulse in the middle of the evolution period was performed with the DANTE sequence.[17] A unique decoupler power setting was used for all the proton pulses (selective and nonselective). The digital resolution in F1 was ±0.3 Hz/point.

Steady-state NOE difference spectra were obtained with irradiation times and pulse intervals greater than 5 times the longest T_1 for the sugar signals. Difference FIDs (512) were accumulated and multiplied with a 1-Hz line-broadening factor prior to Fourier transformation to reduce noise.

(14) Hough, L.; Phadnis, S. P.; Tarelli, E. *Carbohydr. Res.* **1975**, *44*, 37–44.
(15) IUPAC–IUB, Commission on Biochemical Nomenclature. *Arch. Biochem. Biophys.* **1971**, *145*, 405–421; *J. Mol. Biol.* **1970**, *52*, 1–17.
(16) Cremer, D.; Pople, J. A. *J. Am. Chem. Soc.* **1975**, *97*, 1354–1358.
(17) Morris, G. A.; Freeman, R. J. *J. Magn. Reson.* **1978**, *29*, 433–462.
(18) Brown, G. M.; Levy, H. A. *Acta Crystallogr.* **1973**, *B29*, 790–797.
(19) Lipari, G.; Szabo, A. *J. Am. Chem. Soc.* **1982**, *104*, 4546–4559.
(20) Mirau, P. A.; Bovey, F. A. *J. Am. Chem. Soc.* **1986**, *108*, 5130–5134.
(21) (a) Garbi-Benarous, J.; Ladam, P.; Delaforge, M.; Girault, J. P. *J. Chem. Soc., Perkin Trans. 2* **1992**, 1989–2006. (b) Jippo, T.; Kamo, O.; Nagayama, K. *J. Magn. Reson.* **1986**, *66*, 344–348. (c) Hricovini, M.; Tvaroska, I.; Uhrin, D.; Batta, G. *J. Carbohydr. Chem.* **1989**, *8*, 389–394.

Phase-sensitive NOESY[22] were acquired at field strengths of 250.13 and 400.13 MHz with mixing times of 0 and 1 s. A 20-ms variable delay was introduced at the beginning of the mixing time in order to suppress J-peak transfer.[23] The recycle time was set to 5 times the longest T_1 in order to obtain a symmetrical normalized NOESY volume matrix. The diagonal and cross-peak intensities were evaluated from the summed ω_1 subspectra contributing to a specific signal. Each experiment was run twice, and standard (average) deviations[24] were calculated for the cross-peak volumes, $a_{k,l}$ (diagonal volumes, $a_{k,k}$). Integration of noise in these spectra gave ±0.005 units of normalized intensity with respect to the diagonal volume (τ_m = 0 s) for typical peak widths.

Transient 1-D NOEs were measured with the inversion–recovery sequence (180^{sel}–τ–90–FID). The selective 180 pulse was performed with the DANTE-Z pulse scheme,[25,26] and parameters for seven τ values (0.2, 0.3, 0.4, 0.5, 0.6, 0.7, and 0.8 s) were acquired. The experiment was repeated four times. The data points were fitted to the following equation[23] with the SIMPLEX algorithm:[24]

$$f_S\{I\}(\tau) = f_I\{S\}(\tau) = -(\sigma/D)(e^{-(R'+D)\tau} - e^{-(R'-D)\tau})$$

where

$$D = [(1/4)(R_I - R_S)^2 + \sigma_{IS}^2]^{1/2}$$

and

$$R' = (1/2)(R_I + R_S)$$

Conformational Analysis. Rigid (Φ,Ψ) Maps. The initial geometry of sucralose was based on the atomic coordinates taken from the crystal structure.[3] Hydroxylic hydrogen atoms were removed to allow greater flexibility around the glycosidic linkage, and refinement of the C–H bond length was carried out to get more accurate coordinates for the remaining hydrogen atoms. The molecular mechanics calculations were performed using the 5.3 Tripos force field.[27] In order to avoid interference with parameters already in place, new atomic types were created specifically for carbohydrates.[28a,b] The potential energy calculations were performed on 18 starting models (different combinations of side group orientations: GT and TG orientations for ω_g;[29] GG, GT, and TG orientations for ωf and χf). For each model, systematical rotations around the Φ and Ψ angles were performed by scanning the whole angular range in 5° increments. This was carried out by using the SEARCH option of the Sybyl[27] software. In this approach, the two residues are considered as rigid and for each step the conformational energy is evaluated by the Tripos force field. The electrostatic contribution was not taken into account. A set of 18 rigid maps was obtained.

Relaxed (Φ,Ψ) Maps. Because furanoid rings are more flexible than pyranose rings, the use of molecular-modeling programs that allow the bond lengths, bond angles, and torsion angles to relax seems more important for sucrose-based molecules than for disaccharides consisting of two glycopyranose rings. Recent work has shown that the fructofuranose ring is capable of facile puckering, leading to two main low-energy domains separated by only a 2.5-kcal energy barrier.[30]

As with the rigid-map calculations, several starting models have to be considered. For each of the 18 models considered above, a clockwise and a counterclockwise orientation of the secondary hydroxylic groups at OH-2 and OH-3 are needed since the hydroxyl groups may form a partial bonding network around the pyranose ring. Using a recently proposed strategy for automation of flexible-residue conformational analysis,[31] sucralose was analyzed with MM3.[32-35] This procedure drives Φ and Ψ dihedral angles and provides full geometry relaxation through Allinger's MM3 program. Unlike the MM3 DRIVER option, this procedure starts at each step with the same unique residue geometry and not with the optimized coordinates of the preceding conformation. Eliminating the "memory" of the minimization algorithm circumvents the creation of false minima and avoids sudden drops in energy due to important conformational changes in the rest of the molecule. For a given molecule, conformational energy is evaluated by including the partitioned contributions arising from van der Waals and dipolar interactions (with a dielectric constant of 4 as found most appropriate by comparison with carbohydrate crystal structures), potentials for bond stretching, bending, and stretch-bending, a 3-fold torsional potential, and the hydrogen-bonding influence. MM3 also provides for exoanomeric effects.[36] The block-diagonal minimization method, with a default convergence criterion of 3.6 cal/mol, was used for grid-point optimizations. All of the 36 relaxed (Φ,Ψ) maps were constructed with 20° grid spacing; the isoenergy contours were plotted within an 8-kcal range above the global minimum.

Adiabatic Map. Relaxed maps are projections of a multidimensional space in a two-dimensional space. For each (Φ,Ψ) couple there is an infinity of possible arrangements of the molecular internal degrees of freedom (bond length and angles, torsion angles, etc.). Only one of these conformers has the lowest energy and represents a local minimum. A conformational energy map in which only these multiple local minima are plotted as a function of the glycosidic angles will be referred to in this work as an "adiabatic" energy map.[37] Because energy minimization algorithms used in molecular and quantum mechanics programs are incapable of overcoming energy barriers, pertinent starting models have to be chosen to initiate the conformational search procedure. The 36 relaxed maps, accounting for some of the less energy consuming degrees of freedom (the CH_2R rotations), were used to establish an "adiabatic" map as accurate as possible.

Calculations of Coupling Constants, Steady-State NOEs, and the Relaxation Matrix from a Computer Model. Coupling constants, $^3J_{H,H}$, for vicinal hydrogen atoms of a HCCH segment were calculated with the relationship[38]

$$^3J_{H,H} = P1\cos^2(\Theta) + P2\cos(\Theta) + P3 + \sum \Delta\chi_i(P4 + P5\cos^2(\xi_i\Theta + P6|\Delta\chi_i|))$$

which accounts for J dependence on the dihedral angle (Θ) of the HCCH fragment, and on the electronegativity (χ^H, χ^C, χ^O, and χ^{Cl} are 2.20, 2.55, 3.44, and 3.16, respectively)[39] and orientation of the α and β substituents. The fitting parameters P1–P6 and the definition of the sign of the torsion angle (introduced by ξ) are those reported by Haasnoot *et al.*[38] The coupling constant $^3J_{C,H}$ across the glycosidic linkage was calculated by using a recent Karplus-type equation for the COCH segment:[40]

$$^3J_{C,H} = 5.7\cos^2(\Phi^H) - 0.6\cos(\Phi^H) + 0.5$$

where

$$\Phi^H = (H\text{-}1g\text{–}C\text{-}1g\text{–}O\text{-}1g\text{–}C\text{-}2f)$$

As macroscopic properties arise from balanced contribution of each element of an ensemble, averaging of NMR parameters was performed

(22) Macura, S.; Huang, Y.; Suter, D.; Ernst, R. R. *J. Magn. Reson.* **1981**, *43*, 259–281.
(23) Neuhaus, D.; Williamson, M. In *The Nuclear Overhauser Effect in Structural and Conformational Analysis*; VCH Publishers: Cambridge, 1989, p 292.
(24) Press, W. H.; Flannery, B. P.; Teukolsky, S. A.; Vettering W. T. In *Numerical Recipes in Pascal, The Art of Scientific Computing*; Cambridge University Press: Cambridge, 1989.
(25) Boudot, D.; Canet, D.; Brondeau, J.; Boubd, J. C. *J. Magn. Reson.* **1989**, *83*, 428–439.
(26) Poppe, L.; van Halbeek, H. *Magn. Reson. Chem.* **1991**, *29*, 355–361.
(27) Tripos Associates, Inc.: a subsidiary of Evans & Sutherland, St. Louis, Missouri.
(28) (a) Imberty, A.; Hardman, K. D.; Carver, J. P.; Pérez S. *Glycobiology* **1991**, *1*, 631–642. (b) Pérez, S.; Imberty, A.; Meyer, C. In *Separation and Characterization of Complex Oligosaccharides: Determination by MS and NMR Methods*; Reinhold, V., Cumming, D. A., Eds.; Academic Press: Orlando, in press.
(29) Marchessault, R. H.; Pérez, S. *Biopolymers* **1979**, *18*, 2369–2374.
(30) Pérez, S.; Meyer, C.; Imberty, A.; French, A. D. In *Sweet Taste Chemoreception*; Mathlouthi, M., Kanters, J., Birch, Eds.; Elsevier: London and New York, 1993, pp 55–73.
(31) French, A. D.; Tran, V.; Pérez, S. *ACS Symp. Ser.* **1990**, *430*, 191–230.
(32) Allinger, N. L.; Yuh, Y. H.; Lii, J. H. *J. Am. Chem. Soc.* **1989**, *111*, 8551–8566.
(33) Lii, J. H.; Allinger, N. L. *J. Am. Chem. Soc.* **1989**, *111*, 8566–8575.
(34) Lii, J. H.; Allinger, N. L. *J. Am. Chem. Soc.* **1989**, *111*, 8576–8582.
(35) Allinger, N. L.; Rahman, M.; Lii, J. H. *J. Am. Chem. Soc.* **1990**, *112*, 8293–8307.
(36) Pérez, S.; Marchessault, P. *Carbohydr. Res.* **1978**, *65*, 114–120.
(37) Tran, V.; Brady, J. W. *ACS Symp. Ser.* **1990**, *430*, 213–226.
(38) Haasnoot, C. A. G.; de Leeuw, F. A. A. M.; Altona, C. *Tetrahedron* **1980**, *36*, 2783–2792.
(39) Moore, W. J. In *Physical Chemistry*; Longman, Ed.; Harlow, 1972.
(40) Tvaroska, I.; Hricovini, M.; Petrakova, E. *Carbohydr. Res.* **1989**, *189*, 359–362.

Table I. 400-MHz ^{1}H NMR Chemical Shift[a] and Coupling Constant Data of Sucralose in D_2O at 296 K

proton	δ expt	$J_{x,x+1}$ expt[b]	$J_{x,x+1}$ simul[c]	$J_{x,x+1}$ calc[d]
		α-Galp		
H-1	5.48	4.2	4.2	4.0
H-2	3.95	10.4	10.4	9.5
H-3	4.18	3.6	3.6	3.6
H-4	4.53	1.2	1.2	1.5
H-5	4.42	5.5	5.5, 6.0	
H-6, H-6'	3.76	AB	11.5(3.2)	
		β-Fruf		
H-1	3.80	AB	13.0(5.7)	
H-3	4.42	8.4	8.4	8.5
H-4[e]	4.13	8.3	8.3	9.2
H-5[e]	4.08	m	4.5, 7.6	
H-6, H-6'	3.90	AB	11.5(7.8)	

[a] Referenced to internal DMSO (δ 2.72 ppm). [b] Digital resolution of 0.1 Hz/point. [c] Simulation with the Bruker package PANIC. [d] Calculated according to ref 38 for the 11 664 conformers. [e] Not a first-order spin system.

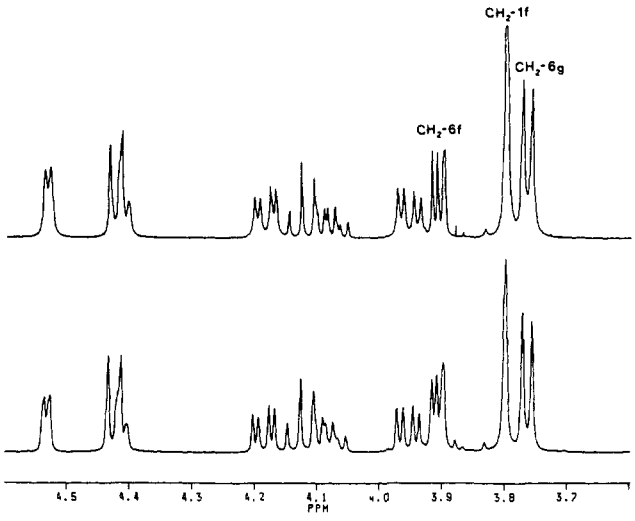

Figure 2. (a, bottom) Experimental and (b, top) simulated 400-MHz ^{1}H NMR spectra of sucralose in D_2O.

on the total population of 11 664 conformers. At a given temperature, the probability of existence (P_i) of the ith conformer depends upon its energy and is governed by a Boltzmann distribution. For a system distributed over n conformational microstates, it follows that

$$P_i = \exp(-E_i/KT)/Q$$

where Q, the classical partition function, is given by

$$Q = \sum\nolimits_n \exp(-E_i/KT)$$

and thus

$$\langle {}^3J_{H,H}\rangle = \sum\nolimits_n P_i {}^3J_{iH,H} \quad \text{and} \quad \langle {}^3J_{C,H}\rangle = \sum\nolimits_n P_i {}^3J_{iC,H}$$

Theoretical NOE values were computed using the full relaxation matrix method. It is necessary to know the rate of conformational exchange in order to account for internal motions in the treatment of NOEs.[41] Both the averaging method and the appropriate spectral density functions depend on the relative rates of overall and internal motion.

In the case of the *rigid-molecule model*, averaging was performed over all values of the inverse sixth power of the interproton distances. Only the conformations having an energy value less than 20 kcal/mol were taken into account in these averaging procedures.

$$\langle r(k,l)^{-6}\rangle = \sum P_i r_i(k,l)^{-6}$$

The ensemble average relaxation matrix was calculated from these

(41) Carver, J. P. *Curr. Opin. Struct. Biol.* **1991**, *1*, 716–720.

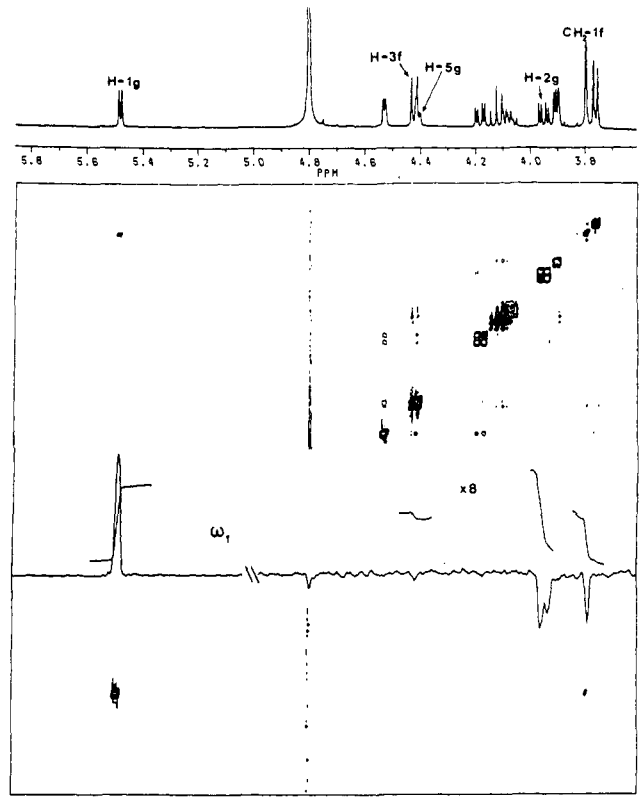

Figure 3. Unsymmetrized, phase-sensitive 400-MHz ^{1}H NOESY spectrum of sucralose in D_2O.

Table II. 100-MHz ^{13}C NMR Data of Sucralose in D_2O at 296 K

carbon	δ[a]	T_1[b] ( )[c]	$^3J_{C,Hx}$ (Hx) expt[d]	$^3J_{C,Hx}$ (Hx) calc[e]
		α-Galp		
C-1	93.96	0.54 (0.29)		
C-2	68.89	0.55 (0.25)		
C-3	69.35	0.58 (0.31)		
C-4	64.31	0.58 (0.33)		
C-5	72.04	0.57 (0.32)	6.6 (H-1g)	
C-6	62.68	0.38 (0.19)		
		β-Fruf		
C-1	44.85	0.28 (0.16)		
C-2	104.65	0.49	3.7 (H-1g)	3.3
C-3	77.35	0.53 (0.33)		
C-4	76.59	0.54 (0.28)		
C-5	82.49	0.49 (0.28)		
C-6	46.11	0.34 (0.20)		

[a] Referenced to internal DMSO (δ 39.5 ppm). [b] 296 K. [c] 283 K. [d] Digital resolution 0.3 Hz/point. [e] According to ref 40.

$\langle r(k,l)^{-6}\rangle$ values using spectral density functions appropriate for a rigid molecule undergoing isotropic motion,

$$J_n(\omega) = \tau_c/(1 + n^2\tau_c{}^2\omega^2)$$

For comparative purposes a set of experimental NOESY volumes was back-transformed[42] to give an experimental relaxation matrix. A uniform leakage coefficient of 14% was added to the diagonal elements in order to account for relaxation to external sources. This correction gave the best fit between the theoretical and experimental relaxation matrices.

Steady-state NOE values were calculated from this relaxation matrix according to the general multispin equation of Noggle and Schirmer.[43] This equation uses a single internuclear vector to describe A_2X interactions, whereas computer models provide internuclear distances pairwise between each methylene proton and all the other spins. Accordingly, NOE values were calculated for all combinations of the theoretical proton positions of the three methylene groups and the eight data sets were averaged.

(42) Olejniczak, E. T.; Gampe, R. T., Jr.; Fesik, S. W. *J. Magn. Reson.* **1986**, *67*, 28–41.

(43) Noggle, J. H.; Schirmer, R. E. In *The Nuclear Overhauser Effect*; Academic Press: New York, 1971.

Table III. Theoretical[a] (Experimental) 400-MHz Steady-State NOEs

	H-1g	H-2g	H-3g	H-4g	H-5g	H-6g	H-1f	H-3f	H-4f + H-5f	H-6f
H-1g		28.5 (20.2)					4.0 (5.1)		0.7 (2.0)	
H-2g	18.7 (15.0)						−2.4 (−3.1)			
H-3g		6.6 (1.7)		12.7 (12.4)	5.7 (9.4)					
H-4g			15.3 (12.8)		6.7 (1.8)	1.1 (3.3)				
H-5g[b]			10.3 (10.1)	10.2 (5.7)		1.5 (3.3)			7.1[c]	
H-6g	0.4 (1.8)	0.8 (3.6)		9.1 (8.2)	10.1 (13.8)					
H-1f	19.9 (20.6)							17.3 (17.8)		
H-3f							2.1 (2.7)		13.8[c] (21.3)	
H-4f + H-5f	0.6 (−2.0)						18.3 (23.2)			3.4 (0.0)
H-6f[d]					5.3 (0.0)		−3.2 (0.0)	35.2 (37.4)		

[a] Average data set (from eight sets of parameters reflecting all combinations of the theoretical positions of the methylene protons) calculated with in-house software according to ref 43. [b] Overlapping signals. [c] Overlapping NOE enhancements. [d] H-2g partially saturated (20%).

In the case of the *flexible-molecule model* the relaxation matrix was calculated from $\langle r(k,l)^{-3}\rangle$ and $\langle r(k,l)^{-6}\rangle$ with spectral density functions appropriate for fast internal motion,[19]

$$J_n(\omega) = \{\bar{S}(k,l)^2\tau_c/(1 + n^2\tau_c^2\omega^2)\} +$$

$$\{(\langle r(k,l)^{-6}\rangle - \bar{S}(k,l)^2)\tau(k,l)/(1 + n^2\,\tau(k,l)^2\omega^2)\}$$

where

$$\bar{S}(k,l)^2 = S(k,l)^2/\langle r(k,l)^3\rangle$$

and

$$\tau(k,l)^{-1} = \tau_e(k,l)^{-1} + \tau_c^{-1}$$

$\bar{S}^2$, which is the generalized order parameter, has been evaluated from the internuclear distance matrix and $S(k,l)^2$, the angular component of motional averaging. τ_c and $\tau_e(k,l)$ are the correlation times for the overall molecular reorientation and the internal motion of the $r(k,l)$ vector, respectively. NOESY volumes were established[42] for the different motional models without correction for leakage to external sources.

Results and Discussion

NMR. The ^{1}H chemical shifts and coupling constants for sucralose in D_2O are collected in Table I. The data, which were extracted from a phase-sensitive 2-D correlation spectrum, are similar to those reported[4] for sucralose in DMSO-d_6. The protons of the methylene groups are more strongly coupled in D_2O (Figure 2a), than in DMSO-d_6. Values of 0.96, 0.92, and 0.83 for the strong coupling parameters of the CH_2-6g, CH_2-1f, and CH_2-6f groups, respectively, were estimated from the simulated spectrum (Figure 2b). Qualitatively, the $^3J_{H,H}$ values are compatible with $^4C_1$ and $^4T_3$ ring forms for the galactopyranosyl[12] and fructofuranosyl[4] residues, respectively. The 100-MHz ^{13}C chemical shifts, heteronuclear three-bond coupling constants, and T_1 values are collected in Table II. Assignments were extracted from the 2-D heteronuclear correlation spectra. The chemical shifts are similar to those of sucrose with the exception of the signals of the carbons substituted by chlorine, which appear at higher field. The experimental value of 3.7 Hz for the interresidue heteronuclear coupling constant, $^3J_{H\text{-}1g,C\text{-}2f}$, is slightly smaller than that of sucrose (4.2 Hz).[12] The T_1 values of the methine carbons are almost identical (the maximum deviations are 5% and 8% at 296 and 283 K, respectively), indicating isotropic motion.

At the onset of this work, it was anticipated that the interpretation of the homonuclear relaxation data would be handicapped by the presence of strong coupling[44a,b] and/or internal motion.[41] It has been suggested that, in the presence of strong coupling, steady-state NOEs are less sensitive to experimental conditions than transient ones. Moreover, the large values of the strong coupling parameters suggested that the pendant groups might be satisfactorily modeled as A_2X systems. Accordingly, these 1-D spectra have been recorded in order to probe the strong coupling effect, and the enhancements are collected in Table III.

The 400.13- and 250.13-MHz NOESY volumes (experimental error: standard deviation for $a_{k,l}$ and average deviation for $a_{k,k}$) are collected in Tables IV and V. In the case of the experiments at 400.13 (250.13) MHz the average value of the standard deviation for the cross-peak volumes is 10% (8%), while that of the diagonal volumes is 0.4% (1.6%). In order to obtain more accurate data for the interactions between H-5g and both interring (H-6f) and intraring (H-6g) methylene protons, the NOE buildups were measured with a transient 1-D experiment (Table VI). The signal-to-noise ratio of the NOESY spectra, Figure 3, was roughly 5 times lower than that obtained with the 1-D transient method. Qualitatively, the homonuclear relaxation data measured with these various methods are in agreement with the ring forms indicated by the coupling constant parameters.[45]

One of the major difficulties in modeling relaxation data of carbohydrates is evaluating the relative rates of molecular tumbling and internal motions.[41] In the case of sucrose-containing molecules, rotation of exocyclic groups, torsion about the glycosidic linkage, and ring puckering of the fructofuranose moiety all have to be considered. Although experimental data have been modeled in an attempt to describe internal dynamics, in the case of disaccharides, relative rates of motion are still very controversial.[9-13,41]

In a recent study,[46] the internal motions of carbohydrates have been probed with both ^{13}C and ^{1}H longitudinal relaxation rates. The difference between the overall tumbling evaluated from the carbon T_1 values, τ_C, and the individual proton correlation times,[20] τ_H, can be interpreted in terms of the value of the initial amplitude factor, $\langle A(0)^2\rangle$, of the spectral density function ($J(\omega) = \langle A(0)^2\rangle$

(44) (a) Keeler, J.; Neuhaus, D.; Williamson, M. P. *J. Magn. Reson.* **1987**, *73*, 45–68. (b) Majumdar, A.; Hosur, R. V. *J. Magn. Reson.* **1990**, *88*, 284–304.

(45) Dais, P.; Perlin, A. S. *Adv. Carbohydr. Chem. Biochem.* **1987**, *45*, 125–168.

(46) Braccini, I.; Hervé du Penhoat, C.; Imberty, A.; Pérez, S. *Int. J. Biol. Macromol.* **1993**, *15*, 52–55.

Table IV. Experimental (Standard Deviation)[a] and Theoretical[b] 400.13-MHz Noramlized NOESY Volumes for Spectra (1-s Mixing Time) of Sucralose

	H-1g	H-2g	H-3g	H-4g	H-5g	H-6g	H-1f	H-3f	H-4f	H-5f	H-6f
H-1g	**0.463**	**–0.080**					**–0.031**				
	(0.003)	(0.007)					(0.003)				
	0.463	–0.062					–0.047				
	0.415	–0.061					–0.041				
	0.545	–0.075					–0.026				
H-2g		**0.634**	**–0.011**								
		(0.005)	(0.003)								
		0.721	–0.015								
		0.688	–0.015								
		0.644	–0.015								
H-3g			**0.534**	**–0.054**	**–0.048**						
			(0.003)	(0.003)	(0.005)						
			0.637	–0.052	–0.038						
			0.597	–0.051	–0.037						
			0.541	–0.055	–0.049						
H-4g				**0.486**	**–0.045**	**–0.021**					
				(0.004)	(0.007)	(0.003)					
				0.557	–0.043	–0.020					
				0.512	–0.041	–0.018					
				0.522	–0.049	–0.010					
H-5g					**0.522**	**–0.015**			**–0.039**[c]		**–0.005**
					(0.013)	(0.001)			(0.002)		(0.002)
					0.566	–0.021			–0.034		–0.011
					0.523	–0.018			–0.033		–0.010
					0.553	–0.010			–0.038		–0.006
H-6g						**0.162**					
						(0.003)					
						0.115					
						0.089					
						0.168					
H-1f							**0.109**	**–0.011**			
							(0.001)	(0.001)			
							0.085	–0.029			
							0.064	–0.026			
							0.131	–0.027			
H-3f								**0.522**	**–0.039**[c]		
								(0.013)	(0.002)		
								0.566	–0.034		
								0.523	–0.033		
								0.553	–0.038		
H-4f									**0.560**		**–0.033**[d]
									(0.000)		(0.004)
									0.655		–0.026
									0.618		–0.025
									0.633		–0.025
H-5f										**0.560**	
										(0.000)	
										0.655	
										0.618	
										0.633	
H-6f											**0.145**
											(0.002)
											0.108
											0.083
											0.152

[a] Experimental values in boldface type and standard deviations in parentheses. The experimental error for the $a_{k,l}$ is the standard deviation of four values. In the case of the $a_{k,k}$, the error is the average deviation. [b] According to ref 19. The theoretical values are as follows (rowwise): (a) rigid-molecule value, (b) flexible-molecule value calculated for $S^2 = 0.9$ and $\tau/\tau_c = 0.1$, and (c) flexible-molecule value calculated for two $S^2(k,l)$ values (0.2 for interactions between ring protons and exocyclic ones; 0.9 for the remaining interactions), a τ_c value of 0.15 ns, and several τ values (0.1 ns for the intracyclic pyranosyl interactions, 0.06 ns for the methylene group and the intracyclic furanosyl ones, and 0.015 ns for the interactions between the ring protons and the exocyclic groups). [c] Cross peaks for H-5g and H-3f with H-4f and H-5f. [d] Cross peaks for H-4f and H-5f with H-6f.

$\tau/(1 + \omega^2\tau^2)$) in certain cases in which distance variations are negligible. This factor is by definition equal to 1 in the case of rigid molecules or those whose internal motions are slow with respect to overall tumbling. The presence of *very* rapid internal motion can be accounted for by a reduction in this initial amplitude factor. Such treatment of internal fluctuations is equivalent to assimilating the initial amplitude factor to the generalized order parameter, $\tilde{S}$, and neglecting the second term (τ_e, correlation time of the internal motion) in Lipari and Szabo's expression,[19]

$$J(\omega) = [\tilde{S}^2\tau_c/(1 + n^2\tau^2\omega^2)] + (1 - \tilde{S}^2)\tau_e/(1 + \tau_e{}^2\omega^2)$$

as has been previously shown to be appropriate for carbon relaxation data of sucrose.[10] The initial amplitude factor cancels out in the evaluation of τ_H, as the correlation times are the result of a ratio of spectral densities. Thus, τ_C is expected to be equal to or less than τ_H depending upon whether internal motions are slow or very fast with respect to molecular tumbling. In a recent study[47] of an aromatic dipeptide where internal rotation about the carbonyl carbon–C_α bond is known[48] to be slow compared to molecular tumbling, these τ_C and τ_H values are very similar (mean deviation of ±12%, seven data points).

(47) Ohassan, H.; Rolando, C.; Hervé du Penhoat, C.; Derouet, C. Manuscript in preparation.

(48) Aharoni, S. M.; Hatfield, G. R.; O'Brien, K. P. *Macromolecules* **1990**, *23*, 1330–1342.

Table V. Experimental (Standard Deviation)[a] and Theoretical[b] 250.13-MHz normalized NOESY Volumes for Spectra (1-s Mixing Time) of Sucralose

	H-1g	H-2g	H-3g	H-4g	H-5g	H-6g	H-1f	H-3f	H-4f	H-5f	H-6f
H-1g	**0.477**	**–0.095**					**–0.035**				
	(0.031)	(0.009)					(0.005)				
	0.440	–0.068					–0.048				
	0.376	–0.071					–0.041				
	0.501	–0.095					–0.028				
H-2g		**0.555**	**–0.021**								
		(0.008)	(0.003)								
		0.705	–0.016								
		0.659	–0.017								
		0.601	–0.019								
H-3g			**0.499**	**–0.076**	**–0.073**						
			(0.001)	(0.003)	(0.003)						
			0.617	–0.057	–0.041						
			0.562	–0.059	–0.041						
			0.491	–0.066	–0.049						
H-4g				**0.479**	**–0.063**	**–0.027**					
				(0.032)	(0.006)	(0.004)					
				0.535	–0.046	–0.022					
				0.474	–0.046	–0.018					
				0.474	–0.059	–0.009					
H-5g					**0.505**	**–0.034**			**–0.063**[c]		**–0.020**
					(0.001)	(0.001)			(0.002)		(0.004)
					0.545	–0.026			–0.037		–0.012
					0.487	–0.024			–0.039		–0.010
					0.511	–0.020			–0.039		–0.006
H-6g						**0.120**					
						(0.017)					
						0.095					
						0.062					
						0.140					
H-1f							**0.093**	**–0.034**			
							(0.018)	(0.001)			
							0.069	–0.026			
							0.043	–0.024			
							0.106	–0.020			
H-3f								**0.505**	**–0.063**[c]		
								(0.001)	(0.002)		
								0.545	–0.037		
								0.487	–0.039		
								0.511	–0.039		
H-4f									**0.562**		**–0.034**[d]
									(0.036)		(0.002)
									0.636		–0.028
									0.583		–0.026
									0.595		–0.025
H-5f										**0.562**	
										(0.036)	
										0.636	
										0.583	
										0.595	
H-6f											**0.096**
											(0.005)
											0.089
											0.057
											0.126

[a] Experimental values in boldface type and standard deviations in parentheses. The experimental error for the $a_{k,l}$ is the standard deviation of four values. In the case of the $a_{k,l}$, the error is the average deviation. [b] According to ref 19. The theoretical values are as follows (rowwise): (a) rigid-molecule value, (b) flexible-molecule value calculated for $S^2 = 0.9$ and $\tau/\tau_c = 0.1$, and (c) flexible-molecule value calculated for two $S^2(k,l)$ values (0.2 for interactions between ring protons and exocyclic ones; 0.9 for the remaining interactions), a τ_c value of 0.15 ns, and several τ values (0.1 ns for the intracyclic pyranosyl interactions, 0.06 ns for the methylene group and the intracyclic furanosyl ones, and 0.015 ns for the interactions between the ring protons and the exocyclic groups). [c] Cross peaks for H-5g and H-3f with H-4f and H-5f. [d] Cross peaks for H-4f and H-5f and H-6f.

The individual proton correlation times of sucralose, 0.29–0.48 ns at 283 K, Table VII, are all greater than the overall tumbling time of 0.22 ns with the exception of H-5g (0.19 ns). However, in the case of sucrose[46] it was shown that the difference between τ_C and τ_H was strongly dependent on the temperature. The τ_H values for H-1g (H-4g) at 277 and 286 K were respectively 3.7 (2.9) and 2.0 (1.7) ns for τ_C values of 2.8 and 1.7 ns. This suggests that, in the case of sucralose, at room temperature the difference between τ_C and τ_H could be quite small. It is necessary to be in the dispersion range of field-dependent relaxation parameters in order to use Mirau and Bovey's method for measuring τ_H, which implies operating at low temperatures in the case of disaccharides. The data available are insufficient for determining the relative rates of motion. However, they suggest that at least in the temperature range 277–296 K the rigid-molecule model would not be appropriate for aqueous sucralose.

Molecular Modeling. Potential Energy Surfaces. Each rigid (Φ,Ψ) map shows a narrow range of flexibility for Φ (60°, 120°), while Ψ covers almost the whole angular range (–180°, 100°). It is outside the scope of the present work to show the 18 different isoenergy surfaces which have been calculated. As a typical map, the one calculated for GT–GT–GG is shown in Figure 4a. Four

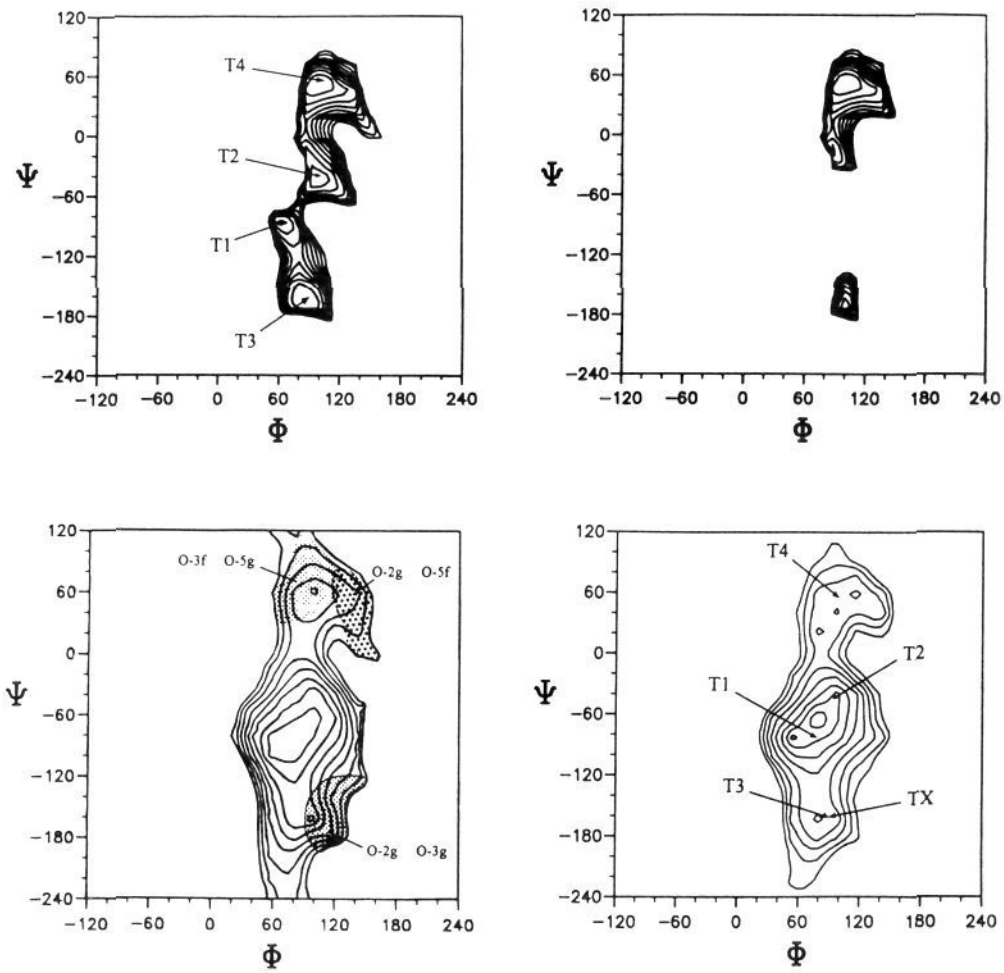

Figure 4. Conformational energy maps for the sucralose disaccharide. (a and b, top) Maps computed with the 5.3 Tripos force field in a rigid-residue manner at 5° of Φ and Ψ torsion angles. The hydroxymethyl and chloromethyl groups were fixed in the GT–GT–GG orientation (referring to ωg–ωf–χf) in map a (left) and GT–GT–GT in map b (right). Isoenergy contours are drawn at increments of 1 kcal/mol with respect to the absolute minimum of the map. (c, bottom left) Map computed with the MM3 force field in a relaxed-residue manner at 20° of Φ and Ψ torsion angles, for ωg = GT, ωf = GT, and χf = GG. Isoenergy contours are drawn by interpolation of 1 kcal/mol above the absolute minimum. (d, bottom right) "Adiabatic" map calculated with MM3 and 36 starting structures (18 different side-group orientations and two patterns of hydroxyl hydrogen orientations) at 20° of Φ and Ψ. Isoenergy contours are drawn by interpolation of 1 kcal/mol above the absolute minimum. The regions giving rise to the occurrence of interresidue hydrogen bonds, O-2g···O-3f, O-3f···O-5g, and O-2g···O-5f, are indicated. The locations of the four low-energy conformers (T1–T4) referred to Φ and Ψ values are labeled on maps a and d. The crystal structure conformation (TX) is also labeled on map d.

Table VI. Experimental (Standard Deviation)[a] and Theoretical[b] 400.13-MHz 1-D Transient NOEs of Sucralose

intracyclic NOEs between H-3f,H-5g and					intercyclic NOE
H-3g	H-2g	H-1f	H-6g	H-1f + H-6g[c]	H-3f,H-5g/H-6f
0.058	**0.010**	**0.036**	**0.076**	**0.112**	**0.018**
(0.016)	(0.008)	(0.006)	(0.006)		(0.008)
0.073	0.005	0.101	0.091	0.192	0.047
0.077	0.005	0.105	0.096	0.201	0.049
0.087	0.006	0.085	0.037	0.122	0.019

[a] Experimental values in boldface type and standard deviations in parentheses. The experimental error for σ_{kl} is the standard deviation of four values. [b] See footnote *b* of Tables IV and V. [c] Overlapping multiplets.

Table VII. The Nonselective Rate, the Selective Rate, and the Correlation Times[a] for the Protons in Sucralose at 283 K

proton	R^{ns} (s^{-1})	R^{s} (s^{-1})	τ_H[b] (ns)	proton	R^{ns} (s^{-1})	R^{s} (s^{-1})	τ_H[b] (ns)
H-1g	0.81	0.91	0.3	H-1f	0.38	0.29	0.48
H-3g	0.90	0.91	0.35	H-3f	0.65	0.58	0.33
H-4g	0.84	0.95	0.29	H-4f	1.13	1.29	0.31
H-5g	0.60	0.85	0.19	H-6f	0.37	0.37	0.42
H-6g	0.37	0.36	0.43				

[a] Calculated according to ref 20. [b] A molecular tumbling time of 0.22 ns was evaluated from the carbon T_1s at 283 K.

low-energy families of conformers can be identified; they are described by the following (Φ,Ψ) locations: T1 (80, –80), T2 (100, –40), T3 (85, –165), and T4 (100, 60). Of the primary hydroxyl group and the two chloromethyl groups, only the position of Cl-1f has much effect on the potential energy surfaces. This is evident from Figure 4b, which shows a potential energy surface for GT–GT–GT. The loss of conformational accessibility observed when χf adopts the GT conformation is such that conformers of the T1 type no longer exist. This observation holds true, although to a lesser extent, for the TG conformation of Cl-1f. This is consistent both with the sucralose crystal structure in which Cl-1f adopts the GG conformation and with the observation that the GT conformation is never observed for χf[12] in sucrose-containing crystal structures.

As expected, the conformational space accessible with the relaxed approach is greater than with the rigid one. Allowing the individual atomic positions to adjust at each increment of the glycosidic linkage torsion angles provides more accurate conformational energies. This method is also more suited for understanding the conformational pathways existing between isolated minima by lowering energy barriers. Nevertheless, the superimposition of the rigid (Figure 4a) and the corresponding relaxed maps (Figure 4c) provides the same location of the low-

energy regions, although calculated with two different molecular mechanics methods. The global population of 11 664 conformers has been taken into account for the assessment of the theoretical NMR values. A grand total of 132 conformers was retained for closer analysis of conformational features. One of these low-energy conformers belonging to the T3 family closely mimics the conformation adopted in the crystalline state[3] where $\Phi = 91.4°$, $\Psi = -162.2°$, $\omega g = 66.9°$, $\omega f = 61.3°$, and $\chi f = -59.2°$.

The "adiabatic map" which represents the synthesis of the 36 individual relaxed potential energy surfaces is shown in Figure 4d; it contains only three main low-energy domains. They include the previously described four families of low-energy conformers within a 2 kcal/mol contour. The global minimum, located at (80°, −60°), is embedded in a broader low-energy region. All minima contributing to the "adiabatic map" have the hydroxyl hydrogens in the counterclockwise orientation. The present map is similar to the one reported by Hooft *et al.*, for sucralose, using the so-called "prudent ascent" method.[7]

Ring Conformations. The puckering parameters were calculated for each of these 132 low energy minima conformers. The pyranoid ring adopts a $^4C_1$ conformation as shown by the average total puckering amplitude Q (0.58) very close to the Q value of an ideal cyclohexane chair ($Q = 0.63$ for R(C–C) = 1.54 Å) and by the average deviation angle θ (3°) close to 0. The furanoid ring is more flexible with ϕ covering the four adjacent $_3E$, $^4T_3$, ^4E, and $^4T_5$ shapes, as indicated by the ϕ values which range from 258° to 303°. This agrees with a previous molecular mechanics study on the fructofuranose ring conformation that showed that the overall minimum and the ^2E, $^2T_3$, $_3E$, $^4T_3$, ^4E, and $^4T_5$ conformations were bound by a 2.5 kcal/mol contour within which facile pseudorotation would be expected.[29] That prediction was supported by the observation that the fructofuranosyl moiety in most crystal structures fell in that range.

Orientation of the CH_2R Groups. No significant departure away from their initial positions was found for ωg, ωf, and χf in the low-energy conformers. However, the main deviations, about 20°, were systematically observed for χf when oriented in the unfavored GT conformation. As a result, these conformers were found to have higher energy.

Interresidue Conformation and Hydrogen Bonding. Molecular drawings representative of the four families of low-energy conformers are shown in Figure 5. For the sake of comparison, the orientation of the hexopyranose residue has been kept fixed in these representations. The occurrence of the O-2g···O-3f hydrogen bond, in the clockwise and the counterclockwise pattern, is found in the (80°, −160°) low-energy region corresponding to the T3 family. From our calculations, there appears to be a systematic preference of about 2–3 kcal/mol for the counterclockwise case. Such an interresidue hydrogen bond between O-2g and O-3f has been shown to occur in the crystal structure and in solution as well. In the crystalline conformation O-2g is the donor; this corresponds to a counterclockwise pattern of OH-2g. On the basis of ^{1}H SIMPLE NMR measurements in DMSO, Christofides *et al.*,[4] suggested the persistence of a strong OH-3f···O-2g hydrogen bond. This would correspond to the occurrence of the "clockwise" pattern. Another interresidue hydrogen bond, OH-3f···O-5g, is predicted to take place when the T4 type of conformation occurs at $\Phi = 100$ and $\Psi = 60$. Marginally, another hydrogen bond may occur (HO-2g···O-5f) for glycosidic conformations in the vicinity of $\Phi = 120$ and $\Psi = 60$; these two hydrogen bonds cannot appear simultaneously (Figure 4c). As for the T1 and T2 families of low-energy conformers, there is no possible interresidue hydrogen bond. In particular the intramolecular O-1f···O-2g bond of sucrose cannot be formed in sucralose because of the chlorine substitution at C-1f. The same is also true for the O-6f···O-5g one, which cannot occur because of the chloride substitution at C-6f.

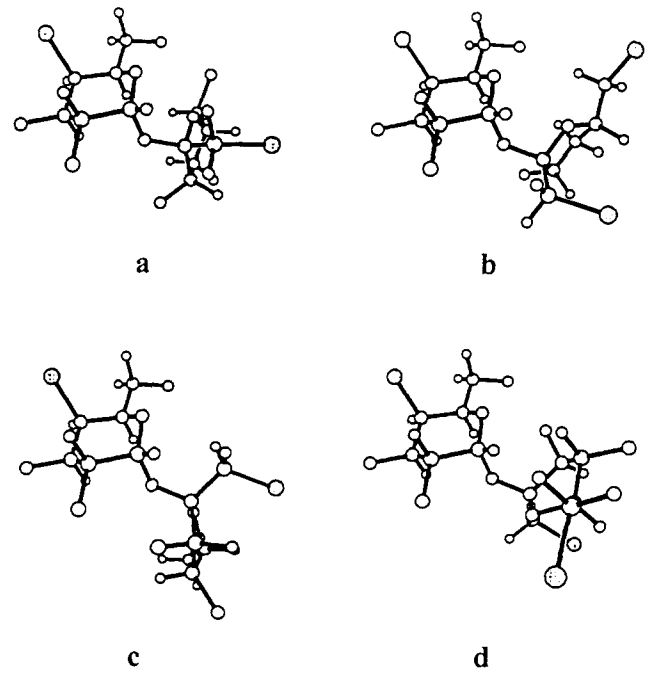

Figure 5. Molecular representation of four low-energy conformations of sucralose. The minima chosen here have all the hydroxymethyl and chloromethyl groups in the same orientation, i.e. ωg = GT, ωf = GT, and χf = GG.

Comparison of the Results of NMR and Molecular Mechanics. Coupling Constant Data. $^3J_{H,H}$ values have been calculated for the Boltzmann distribution of the 11 664 conformers as described above (Table I). Mean deviations of 0.4 and 0.5 Hz between theoretical and experimental $^3J_{H,H}$ values indicate an adequate description of the conformations taken by the 4-chloro-4-deoxy-*galacto*-pyranose and 1′,6′-deoxy-1′,6′-dichlorofructofuranosyl residues. As regards the orientation about the glycosidic linkage, the heteronuclear three-bond H-1g/C-2f coupling constant of 3.7 Hz is well-modeled by the value of 3.3 Hz calculated for the average structure.

Rigid-Molecule Relaxation Data. Molecular tumbling times of 0.088 and 0.22 ns at 296 and 283 K, respectively, have been established for the rigid-molecule regime from the corresponding T_1 data. Both steady-state and transient 400.13-MHz NOEs have been modeled using spectral densities appropriate for rigid molecules undergoing isotropic overall reorientation with a correlation time of 0.088 ns and Boltzmann-averaged distances (Tables III and IV). The mean deviations for both these steady-state and transient NOEs (interactions with S/N > 2) are high, 31 and 26%, respectively. A poorer fit is observed in both cases if one considers only the interactions with the pendant groups, 35% (steady-state NOEs) and 98% (transient NOEs). Both the higher signal-to-noise ratio of the steady-state experiments compared to that of the 2-D transient ones and the more favorable treatment of NOEs in the presence of strong coupling might explain why this latter deviation is lower in the case of the steady-state experiments. It should be noted that the theoretical steady-state interresidue NOEs, $f_{H\text{-}1f}\{H\text{-}1g\}$ and $f_{H\text{-}1g}\{H\text{-}1f\}$, are in good agreement with the experimental values, 4.0% for 5.1% and 19.9% for 20.6%, respectively. The interglycosidic effects between H-5g and H-6f were not detected. On the whole, the fit between the rigid-molecule simulations and the relaxation data of sucralose is mediocre.

Flexible-Molecule Relaxation Data. In the case of the flexible-molecule treatment, a range of overall correlation times, τ_c, was evaluated from plots of T_1^{-1} (methine carbons, 296 K) versus τ_c for order parameters ranging from 0.4 to 0.9 and τ/τ_c ratios of 0.01, 0.1, and 0.5. For example, correlation times of 0.12, 0.17, and 0.26 ns were obtained for S^2 values of 0.9, 0.6, and 0.4 and

Table VIII. Average Standard Deviations of Theoretical 400.13-MHz (250.13-MHz) NOESY Normalized Volumes for a Spectrum of Sucralose Acquired with a 1-s Mixing Time

dynamic model	$a_{k,l}$[a] > 2(S/N)	$a_{k,l}$[a] > 4(S/N)	$a_{k,l}$[b] for methine protons	$a_{k,k}$
rigid	26 (29)	18 (29)	13 (32)	18 (16)
$S^2 = 0.9$	26 (28)	19 (28)	16 (29)	23 (25)
$S^2 = 0.2, S^2 = 0.9$	26 (25)	14 (25)	4 (17)	9 (11)

[a] Averaged experimental standard deviation for all $a_{k,l}$ values is 10% (8%). [b] Averaged experimental deviation for all $a_{k,k}$ values is 0.4% (1.6%).

a τ/τ_c ratio of 0.1, respectively. This latter ratio also has a strong influence on the overall tumbling parameter as a value of 0.14 ns is estimated for $S^2 = 0.6$ and $\tau/\tau_c = 0.3$. Order parameters of 0.89, 0.67, 0.72, and 0.76 have been established for the hydroxymethyl carbons, C-6f, C-6g, and C-1f of sucrose by McCain and Markley.[9,10] A slightly higher value, 0.94, was reported for the ring carbons of sucrose in a more viscous medium.[11]

The 250.13- and 400.13-MHz theoretical NOESY volumes were simulated for a wide range of molecular tumbling times (0.088–0.26 ns), order parameters (0.2–1.0), and τ_e ($0.01\tau_c$–$0.8\tau_c$) values, and some of these data are collected in Tables IV and V. Mean standard deviations for three (*vide infra*) of these dynamic models are collected in Table VIII. In the case of overlapping multiplets (H-3f/H-5g, H-4f/H-5f, and the methylene groups) the summed normalized volumes are indicated. Cross peaks have been attributed to a particular pair of spins only if the other internuclear distances are greater than 5 Å. It is to be noted that the spectral dispersion of the 400.13-MHz NOESY experiments is much more favorable than that of the 250.13-MHz ones.

The average deviation (%) for the rigid-molecule simulation at 400.13 (250.13) MHz was 26 (29), 18 (29), and 13 (32) when taking into account $a_{k,l}$ values with S/N ratio >2, >4, and all values not involving exocyclic groups, respectively. When unique S^2 values and a τ/τ_c ratio of 0.1 are used in connection with flexible-molecule spectral density functions, the best fit (%), 26 (28), 19 (28), and 16 (29) for the cross-peak volumes enumerated above, was obtained for $S^2 = 0.9$ and $\tau_e = 0.12$ ns. However, a calculation with $S^2(k,l)$ values of 0.2 for interactions between ring protons and exocyclic groups and 0.9 for the remaining ones, a τ_c value of 0.15 ns, and τ values optimized for the various groups (0.1 ns for the intracyclic pyranosyl interactions, 0.06 ns for the methylene group and the intracyclic furanosyl ones, and 0.015 ns for interactions between the ring protons and the exocyclic groups) gave the best agreement between experimental and simulated cross-peak volumes (%): 26 (25), 14 (25), and 4 (17) for the cross-peak volumes previously enumerated. For these three simulations the average deviations (%) of the diagonal volumes are 18 (16), 23 (25), and 9 (11), respectively.

Ideally, all the calculated volumes should be slightly larger than the experimental ones as relaxation due to mechanisms other than intramolecular dipolar interactions has been neglected. When all volumes with a S/N ratio greater than 2 are considered, all three dynamic models give the same average standard deviation due to the mediocre fit of the weakest cross peaks. In all cases, the fit is greatly improved when volumes involving the methylene protons are neglected. As previously stated, this could be the result of strong coupling, an inadequate model for the internal motion, and/or the low intensity of these cross peaks. Considering the experimental precision of the $a_{k,l}$ (average standard deviation of 10% (8%)) and $a_{k,k}$ (average deviation of 0.4% (1.6%)) data, the improvement in the fit for the third set of conditions is significant. Moreover, most of the theoretical volumes are slightly larger than the experimental ones.

The relative values of the H-1g/H-2g intracyclic and the H-1g/H-1f interglycosidic transient NOEs are strongly influenced by the motional parameters. For simulations either in the absence of motion or in the presence of rapid motion about the glycosidic linkage, the theoretical values for these two interactions are similar (e.g., $a_{\text{H-1g/H-2g}} = 0.062$ or 0.061 and $a_{\text{H-1g/H-1f}} = 0.047$ or 0.041 at 400.13 MHz). The ratio of the experimental amplitudes for these two interactions is much closer to 3/1. Only the simulations with similar rates of motion for the overall tumbling and glycosidic torsions reproduce these NOESY volumes. A second interglycosidic interaction was probed with NOE buildup data. The experimental relaxation rates for the H-5g/H-6g (the summed H-3f,H-5g/H-6g and H-3f,H-5g/H-1f must be considered due to poor spectral dispersion) and the H-5g/H-6f interactions and the theoretical ones for the motional models given above are collected in Table VI. Both of these data are sensitive to the relative rates of motion and corroborate the dynamic model elaborated from the NOESY volumes.

It should be noted that although a wide variety of motional models may produce the same relaxation rates for several of the dipolar interactions, it does not necessarily follow that the volume matrices will be analogous. The latter data set ($a_{k,l}$) depends on the relaxation matrix as a whole and is thus a much tougher test of dynamic models. Strictly speaking, the spectral density expressions of Lipari and Szabo are exact[49] with basically no restriction on the magnitude of τ_e or τ_c if $S^2 > 0.3$. However, similar results were obtained for other order parameter combinations (0.3 and 0.9; 0.4 and 0.9, etc.), although the fit was slightly poorer. In a recent study of internal motion in two disaccharides, two distinct ratios of relaxation data (NOEs and relaxation rates) at two field strengths (300/500) were observed for interactions modulated by rigid (higher ratio) or fluctuating (lower ratio) distances.[50] Although the same general tendency is observed in this work, both the experimental and theoretical ratios (250.13/400.13) of the $a_{k,l}$ values in Tables IV and V are more disperse [expt (calc) (%): 1.2 (1.3), 1.1 (1.1), 1.4 (1.4), 1.0 (1), 1.4 (1.2), and 1.5 (1) for the H-1g/H-2g, H-1g/H-1f, H-3g/H-4g, H-5f/H-6f, H-4g/H-5g, and H-3g/H-5g interactions, respectively].

It is to be noted that the results from the present study are in contradiction with the extremely fast rate of torsion about the glycosidic linkage of sucrose,[13] which has been recently obtained from homonuclear cross-relaxation rates for a wide range of frequency and temperatures. They also disagree with simulations of the relaxation rates of the protons of methyl β-mannobioside and methyl β-xylobioside at two field strengths where again glycosidic torsions were considered to be 10 times faster than overall tumbling.[50] However, they are in agreement with the absence of interwell transitions about the glycosidic linkage in a recent molecular dynamics simulation of aqueous maltose.[51]

In contrast, the dynamic model reported here is in agreement with the data previously described for hydroxymethyl group rotation. It has been shown[10] from ^{13}C data (relaxation is essentially modulated by the "fixed" C–H distance) that the internal motion of the hydroxymethyl groups of sucrose is restricted (order parameters of 0.67–0.76 at 20 °C for the carbons) with similar motional amplitudes. In a ^{13}C study in the dispersion range, Kovac *et al.*[11] evaluated the difference in the rates of overall tumbling and methyl rotation of a disaccharide to be a factor of 8 at 30 °C. In the molecular dynamics simulation of aqueous maltose, the time interval between two transitions about the exocyclic bonds was roughly 50–60 ps.

Finally, ring puckering of the fructofuranosyl ring has been described as very fast[9] as compared to overall motion from ^{13}C relaxation studies[9] of sucrose. However, again molecular dynamics simulations of sucrose[52] showed that transitions between

(49) Lipari, G.; Szabo, A. *J. Am. Chem. Soc.* **1982**, *104*, 4559–4570.
(50) Hricovini, M.; Shah, R. N.; Carver, J. P. *Biochemistry* **1992**, *31*, 10018–10023.
(51) Brady, J. W.; Schmidt, R. K. *J. Phys. Chem.* **1993**, *97*, 958–966.
(52) Tran, V. H.; Brady, J. W. *Biopolymers* **1990**, *29*, 977–997.

puckering families of conformers are infrequent, suggesting that only low-amplitude motions are very fast compared to molecular tumbling.

Conclusions

The present work shows that sucralose displays a variety of conformations. The occurrence of these conformations, either in the solid state or in dilute aqueous solution, can be understood satisfactorily through the contribution of molecular-modeling studies using the flexible-residue approximation. The observed flexibility of the fructofuranose ring has been successfully rationalized, and the NMR data are explained. A disparity in the observed ranges of Φ and Ψ has been predicted with much greater freedom of rotation about the O-1g–C-2f bond than about C-1g–O-1g bond. This can be partially attributed to the fact that the O-1g–C-2f bond is pseudoequatorial. Furthermore, the mobility of the bulky chlorine substituent at C-1f has been shown to be fairly restricted.

Significant differences are observed between the conformation taken by sucrose and sucralose in their crystalline states. Actually, the structural features that crystalline sucrose exhibits cannot occur for crystalline sucralose. In constrast the crystalline conformation of sucralose about Φ and Ψ is one of the low-energy conformers for sucrose. However, the adiabatic map computed for sucralose bears some similarity to the corresponding map for sucrose. This is an indication that the solution behavior of the two molecules may be quite comparable.

At the present time, the experiments on sucrose and sucralose have not determined the conformations that these molecules would adopt when interacting with sweet receptors such as the transmembrane protein. It is indeed known that, upon binding to a protein, carbohydrates can adopt arrangements that correspond to higher intramolecular energy, as a result of van der Waals and hydrogen-bonding interactions. However, these "high-energy" conformers always belong to low-energy regions of the corresponding potential energy surfaces.[53] In the absence of studies of the active site complex with sucrose or other sweeteners, unraveling some of the essential features associated with the "active states" and the glucophores of these sweeteners can only be approached by establishing structure–activity relationships of a series of molecules having different sweetness qualities.

Acknowledgment. This work was supported by a grant to one of us (C.M.) from Beghin-Say. The provision of financial support by P. et M. Curie University, CNRS (URA 1679), and INRA is acknowledged. The authors would like to express their appreciation to Dr. A. Imberty for helpful discussions.

(53) Imberty, A.; Delage, M. M.; Bourne, Y.; Cambillau, C.; Pérez, S. *Glycoconjugate J.* **1991**, *8*, 456–483.